Cylindrical and spherical Gardner solitons and double layers in a dusty electronegative non-thermal plasma with two-temperature electrons

T. Akhter[a], M. M. Hossain[b)†], and A. A. Mamun[a)]

[a)] *Department of Physics, Jahangirnagar University, Savar, Dhaka-1342, Bangladesh*

[b)] *Department of Electrical and Electronic Engineering, Bangladesh University of Business and Technology, Dhaka-1216, Bangladesh*

(Received 24 October 2012; revised manuscript received 11 December 2012)

A precise theoretical investigation has been made on the cylindrical and spherical (nonplanar) Gardner solitons (GSs) and double layers (DLs) in a dusty electronegative plasma (composed of inertial positive and negative ions, Maxwellian cold electrons, non-thermal hot electrons, and negatively charged static dust). The reductive perturbation method has been used in derivation of the modified Gardner (MG) equation describing the nonlinear propagation of the dust ion-acoustic (DIA) waves. The MG equation admits solitary waves (SWs) and DLs solutions for σ around its critical value σ_c (where σ_c is the value of σ corresponding to the vanishing of the nonlinear coefficient of the Korteweg de-Vries (K–dV) equation). The nonplanar SWs and DLs solutions are numerically analyzed and the parametric regimes for the existence of the positive as well as negative SWs and negative DLs are obtained. The basic features of nonplanar DIA SWs and DLs, which are found to be different from planar ones, are also identified. The implications of our results to different space and laboratory dusty plasma situations, are discussed.

Keywords: electronegative plasma, two-temperature electrons, Garner solitons, double layers

PACS: 52.27.Cm, 52.35.Fp, 52.35.Mw **DOI:** 10.1088/1674-1056/22/7/075201

1. Introduction

Plasmas with a significant amount of negative ions whose contribution cannot be neglected in any way, are known as electronegative plasmas (ENPs).[1–7] ENPs have attracted a great deal of attention not only because of their potential applications in microelectronic and photoelectronic industries[8] but also because of their occurrence in both laboratory devices,[9–11] and space environments.[12–14] The ENPs observed in both space and laboratory devices, are not pure in general. They are contaminated by solid impurities (dust), which are not practically neutral but are charged[15] by absorbing ENP electrons and positive as well as negative ions.[16,17] Therefore, ENPs are also called dirty or dusty ENPs (DENPs).[16–18]

Ghim and Hershkowitz have verified this mode of plasma propagation by a recent laboratory experiment.[19] The nonlinear features of the dust-ion-acoustic (DIA) waves in DENP have been analyzed by various authors,[18–22] and have shown that under suitable plasma conditions, such a plasma can support the existence of solitary structures with both positive and negative potentials.

Cairns *et al.*[23] have considered a non-thermal plasma model and shown that the presence of a non-thermal distribution of electrons may change the nature of ion sound solitary structures and allow the existence of structures very like those observed in upper ionosphere by the Freja and Viking satellites.[24,25] Gill *et al.*[26] have studied the IA solitons and double layers in a plasma consisting of positive and negative ions with non-thermal electrons using small amplitude approximation. Sabry *et al.*[27] considered positive–negative ions and non-thermal electrons, and investigated the properties of ion-acoustic solitary waves (IA-SWs) by employing the pseudopotential approach. Recently, Hussain *et al.*[22] have studied ion acoustic solitons in planar and non-planar geometries in electronegative with non-thermal electrons.

To some extent, all the above mentioned plasma models are simplified since the interaction of multiple electrons (i.e., two-temperature electron) which describes more generalized plasma, were not considered by them. Jones *et al.*[28] first investigated the effects of two temperature electrons in linear approximation for the ion-acoustic waves. They investigated the wave dynamics in a three component plasma consisting of cold ions, and two types of electrons including different thermal effects. Many authors have studied the effects of two-temperature electrons on ion-acoustic solitary structure.[29] The interaction of two types of electron populations, namely, cold and hot, are present in many space observations, such as in the cusp and the auroral field lines,[30] Bohm sheath criterion,[31] auroral region,[32,33] NLCs in Earths atmosphere,[34] etc. Electrons at two different temperatures have also been encountered in laboratory devices such as in double-plasma machines,[35] hot turbulent strong plasmas of thermonuclear,[36,37] hot cathode discharges,[38] and sputtering magnetron plasma.[39]

†Corresponding author. E-mail: manir_phys@yahoo.com

© 2013 Chinese Physical Society and IOP Publishing Ltd

All of these previous studies[18–22,26–29,32,33] are limited to the study of the Korteweg de-Vries (K–dV) or Burger equation describing the solitary or shock waves, but not with Gardner solitons (GSs) and double layers (DLs). However, the K–dV and Burgers equations, which are derived for solitary or shock waves, are not valid for a parametric regime corresponding to $A = 0$ or $A \sim 0$ (where A is the coefficient of the nonlinear term of the K–dV or Burger equation). Moreover, the above mentioned studies are limited to one-dimensional (1D) planar geometry, which may not be the realistic situation in space and laboratory devices, since the waves observed in space (laboratory devices) are certainly not infinite (unbounded) in one-dimension.[40] A technique of analyzing SWs and DLs, is the Gardner approach which leads to a modified Gardner (MG) equation.[41–43] From the numerical analysis of the MG equation, permanent profile SW is found, which is known as a Gardner soliton (GS).[44–50] Recently, many authors have successfully studied the nature of the GS,[44–51] which is found in the vicinity of some critical parameters as well as near $A = 0$.

Therefore, in our present work, we are going to analyze the nonplanar (which is valid for both cylindrical and spherical geometries) DIA SWs and DLs in a DENP system (consisting of positive and negative ions, Maxwellian cold electrons, non-thermal hot electrons, and negatively charged static dust) by using by the reductive perturbation method.[52]

The paper is organized as follows. The governing equations are provided in Section 2. The MG equation is derived by using the reductive perturbation method in Section 3. The numerical analysis is presented in Section 4. A brief discussion is finally given in Section 5.

2. Governing equations

We consider the nonlinear propagation of the DIA waves in an unmagnetized DENP containing inertial positive and negative ions, Maxwellian cold electrons, non-thermal hot electrons, and negatively charged static dust. Thus, at equilibrium, we have $Z_p n_{p0} = Z_n n_{n0} + n_{e10} + n_{e20} + Z_d n_{d0}$, where n_{p0}, n_{n0}, n_{e10}, n_{e20}, and n_{d0}, are, respectively, positive ion, negative ion, non-thermally distributed electron, Blotzmann distributed electron, and negative dust number density at equilibrium. The Z_p (Z_n) represents the charge state of the positive (negative) ion. The number densities of two-temperature non-thermal electrons, n_{e1} and n_{e2},[23,28] are given by

$$n_{e1} = n_{e10}\left[1+\beta\left(\frac{e\phi}{T_{e1}}\right)+\beta\left(\frac{e\phi}{T_{e1}}\right)^2\right]e^{(e\phi/T_{e1})},$$

$$n_{e2} = n_{e20}\,e^{(e\phi/T_{e2})}.$$

We are interested in examining the nonlinear propagation of a low phase speed (in comparison with electron and ion thermal speeds) perturbation mode on the time scale of the DIA waves. The time scale of the DIA waves is much faster than the dust plasma period so that dust can be assumed stationary. This model is relevant to dusty plasmas in the noctilucent cloud region in Earths atmosphere,[34] at the edges of the Auroral Kilometric Radiation source region,[53] double-plasma machines,[37] hot turbulent thermonuclear plasma,[37] rf discharge plasma,[54] etc., where electrons of different kinds involving thermal effects are the major plasma species. The nonlinear dynamics of these low-frequency (purely electrostatic) DIA waves in such a plasma system, whose phase speed is much smaller (larger) than the electron (ion) thermal speed is described by the normalized equations in the form of

$$\frac{\partial n_s}{\partial t}+\frac{1}{r^\nu}\frac{\partial}{\partial r}(r^\nu n_s u_s)=0, \tag{1}$$

$$\frac{\partial u_p}{\partial t}+u_p\frac{\partial u_p}{\partial r}=-\frac{\partial \phi}{\partial r}, \tag{2}$$

$$\frac{\partial u_n}{\partial t}+u_n\frac{\partial u_n}{\partial r}=\mu\frac{\partial \phi}{\partial r}, \tag{3}$$

$$\frac{\partial^2\phi}{\partial r^2}=-\rho, \tag{4}$$

$$\rho = n_p-\mu_1(1+\beta\phi+\beta\phi^2)\,e^{\phi}-\mu_2\,e^{\sigma\phi}-\eta n_n-\mu_d, \tag{5}$$

where $\nu = 0$ for 1D planar geometry, and $\nu = 1$ (2) for a nonplanar cylindrical (spherical) geometry, $\eta = 1-\mu_1-\mu_2-\mu_d$, n_s is the number density of the species s ($s = p$ for positive ions, $s = n$ for negative ions, $s = e1$ for non-thermal electron, and $s = e2$ for Blotzmann distributed electron) normalized by its equilibrium value n_{s0}, u_p (u_n) is the positive (negative) ion fluid speed normalized by $C_p = (Z_p k_B T_{e1}/m_p)^{1/2}$, ϕ is the electrostatic wave potential normalized by T_{e1}/e, ρ is the normalized surface charge density, $\mu = Z_n m_p/Z_p m_n$, $\mu_1 = n_{e10}/Z_p n_{p0}$, $\beta = 4\alpha/(1+3\alpha)$; α being the parameter that determines the population of the non-thermal electrons, $\mu_2 = n_{e20}/Z_p n_{p0}$, $\mu_d = Z_d n_{d0}/Z_p n_{p0}$, $Z_n n_{n0}/Z_p n_{p0} = 1-\mu_1-\mu_2-\mu_d$, and $\sigma = T_{e1}/T_{e2}$. It must be added here that T_{e1} (T_{e2}) is the lower (higher) electron temperature, k_B is the Boltzmann constant, and e is the magnitude of the electron charge. The time variable t is normalized by $\omega_p^{-1} = (m_p/4\pi n_{p0} Z_p^2 e^2)^{1/2}$, and the space variable x is normalized by $\lambda_{Dm} = (k_B T_{e1}/4\pi n_{p0} Z_p e^2)^{1/2}$. We are interested in the propagation of a purely electrostatic perturbation mode on the time scale of the IA waves. Thus, the frequency of this perturbation mode is much higher than the dust-plasma-frequency. Therefore, dust are assumed to be stationary.[55–57]

3. Derivation of MG equation

To study GSs by analyzing the ingoing solutions of Eqs. (1)–(5), we first introduce the stretched coordinates:[42,58]

$$\zeta = \varepsilon(r - V_p t), \tag{6}$$

$$\tau = \varepsilon^3 t, \tag{7}$$

where ε is a small parameter ($0<\varepsilon<1$) measuring the weakness of the dispersion, and $V_{\rm p}$ (normalized by $C_{\rm p}$) is the phase speed of the perturbation mode and expand all the dependent variables (i.e., $n_{\rm s}$, $u_{\rm s}$, ϕ, and ρ) in power series of ε

$$\begin{aligned} n_{\rm s} &= 1+\varepsilon n_{\rm s}^{(1)}+\varepsilon^2 n_{\rm s}^{(2)}+\varepsilon^3 n_{\rm s}^{(3)}+\cdots,\\ u_{\rm s} &= 0+\varepsilon u_{\rm s}^{(1)}+\varepsilon^2 u_{\rm s}^{(2)}+\varepsilon^3 u_{\rm s}^{(3)}+\cdots,\\ \phi &= 0+\varepsilon \phi^{(1)}+\varepsilon^2 \phi^{(2)}+\varepsilon^3 \phi^{(3)}+\cdots,\\ \rho &= 0+\varepsilon \rho^{(1)}+\varepsilon^2 \rho^{(2)}+\varepsilon^3 \rho^{(3)}+\cdots. \end{aligned} \tag{8}$$

Now, expressing Eqs. (1)–(5) in terms of ζ and τ, and substituting Eq. (8) into the resulting equations, one can easily develop different sets of equations in various powers of ε. To the lowest order in ε, one obtains

$$u_{\rm p}^{(1)}=\frac{\psi}{V_{\rm p}},\quad n_{\rm p}^{(1)}=\frac{\psi}{V_{\rm p}^2},\quad \rho^{(1)}=0, \tag{9}$$

$$u_{\rm n}^{(1)}=-\frac{\mu}{V_{\rm p}}\psi,\qquad n_{\rm n}^{(1)}=-\frac{\mu}{V_{\rm p}^2}\psi, \tag{10}$$

$$V_{\rm p}^2=\frac{1+\eta\mu}{\mu_1+\mu_1\beta+\sigma\mu_2}, \tag{11}$$

where $\psi=\phi^{(1)}$. Equation (11) represents the linear dispersion relation for the DIA waves propagating in a dusty plasma under consideration. To the next higher order in ε, we obtain a set of equations, which, after using Eqs. (9)–(11), can be simplified as

$$u_{\rm p}^{(2)}=\frac{\psi^2}{2V_{\rm p}^3}+\frac{\phi^{(2)}}{V_{\rm p}},\qquad n_{\rm p}^{(2)}=\frac{3\psi^2}{2V_{\rm p}^4}+\frac{\phi^{(2)}}{V_{\rm p}^2}, \tag{12}$$

$$u_{\rm n}^{(2)}=\frac{\mu^2\psi^2}{2V_{\rm p}^3}-\frac{\mu\phi^{(2)}}{V_{\rm p}},\ n_{\rm n}^{(2)}=\frac{3\mu^2\psi^2}{2V_{\rm p}^4}-\frac{\mu\phi^{(2)}}{V_{\rm p}^2}, \tag{13}$$

$$\rho^{(2)}=\frac{1}{2}A\psi^2=0, \tag{14}$$

$$A=\frac{3}{V_{\rm p}^4}-\frac{3\eta\mu^2}{V_{\rm p}^4}-\mu_1-4\mu_1\beta-\mu_2\sigma^2. \tag{15}$$

It is clear from Eq. (14) that $A=0$ since $\psi\neq 0$. It is obvious that equation (14) is satisfied for $\sigma=\sigma_{\rm c}$ (critical value of σ).

We have numerically shown how $\sigma_{\rm c}$ varies with μ and α. The results are displayed in Fig. 1 which in fact represents the $A=0$ surface plot, and provides us the parametric regimes (which correspond to the regime above or below the $A=0$ surface plot) of our present interest.

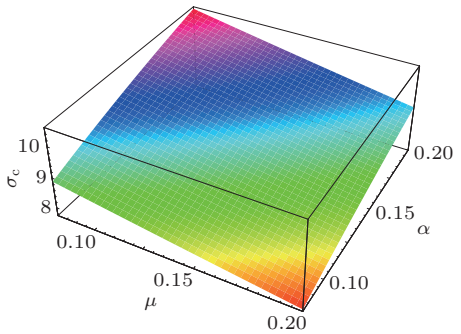


Fig. 1. (color online) Variation of $\sigma_{\rm c}$ (obtained from $A(\sigma=\sigma_{\rm c})=0$) with μ and α for $\mu_1=0.4$, $\mu_2=0.2$, and $\mu_{\rm d}=0.1$.

Hence, for σ around its critical value $\sigma_{\rm c}$, $A=A_0$ can be expressed as

$$A_0\simeq s\left(\frac{\partial A}{\partial\sigma}\right)_{\sigma=\sigma_{\rm c}}|\sigma-\sigma_{\rm c}|=sA_\sigma\varepsilon, \tag{16}$$

where $A_\sigma=\partial A/\partial\sigma$, $s=1$ for $\sigma>\sigma_{\rm c}$ and $s=-1$ for $\sigma<\sigma_{\rm c}$. Then, for $\sigma\neq\sigma_{\rm c}$, we can express $\rho^{(2)}$ as

$$\rho^{(2)}\simeq\frac{1}{2}s\varepsilon A_\sigma\psi^2. \tag{17}$$

This means that for $\sigma\neq\sigma_{\rm c}$, $\rho^{(2)}$ must be included in the third-order Poisson's equation.

To the next higher order of ε, we obtain a set of equations as

$$\frac{\partial n_{\rm p}^{(1)}}{\partial\tau}-V_{\rm p}\frac{\partial n_{\rm p}^{(3)}}{\partial\zeta}+\frac{\partial F_{\rm p}}{\partial\zeta}+\frac{\nu}{V_{\rm p}\tau}u_{\rm p}^{(1)}=0, \tag{18}$$

$$\frac{\partial n_{\rm n}^{(1)}}{\partial\tau}-V_{\rm p}\frac{\partial n_{\rm n}^{(3)}}{\partial\zeta}+\frac{\partial F_{\rm n}}{\partial\zeta}+\frac{\nu}{V_{\rm p}\tau}u_{\rm n}^{(1)}=0, \tag{19}$$

$$\frac{\partial u_{\rm p}^{(1)}}{\partial\tau}-V_{\rm p}\frac{\partial u_{\rm p}^{(3)}}{\partial\zeta}+\frac{\partial}{\partial\zeta}\left[u_{\rm p}^{(1)}u_{\rm p}^{(2)}\right]+\frac{\partial\phi^{(3)}}{\partial\zeta}=0, \tag{20}$$

$$\frac{\partial u_{\rm n}^{(1)}}{\partial\tau}-V_{\rm p}\frac{\partial u_{\rm n}^{(3)}}{\partial\zeta}+\frac{\partial}{\partial\zeta}\left[u_{\rm n}^{(1)}u_{\rm n}^{(2)}\right]-\mu\frac{\partial\phi^{(3)}}{\partial\zeta}=0, \tag{21}$$

$$\begin{aligned} &\frac{\partial^2\psi}{\partial\zeta^2}+\frac{1}{2}sA_\sigma\psi^2+n_{\rm p}^{(3)}-\eta n_{\rm n}^{(3)}\\ &-(\mu_1+\mu_1\beta+\mu_2\sigma)\phi^{(3)}-(\mu_1+4\mu_1\beta+\mu_2\sigma^2)\psi\phi^{(2)}\\ &-\left(\frac{\mu_1}{6}+\frac{3\mu_1\beta}{2}+\frac{\mu_2\sigma^3}{6}\right)\psi^3=0, \end{aligned} \tag{22}$$

where $F_{\rm n}=n_{\rm n}^{(1)}u_{\rm n}^{(2)}+n_{\rm n}^{(2)}u_{\rm n}^{(1)}+u_{\rm n}^{(3)}$ and $F_{\rm p}=n_{\rm p}^{(1)}u_{\rm p}^{(2)}+n_{\rm p}^{(2)}u_{\rm p}^{(1)}+u_{\rm p}^{(3)}$. Now, combining Eqs. (10)–(13) and Eqs. (18)–(22), we obtain

$$\frac{\partial\psi}{\partial\tau}+\frac{\nu}{2\tau}\psi+p\psi\frac{\partial\psi}{\partial\zeta}+q\psi^2\frac{\partial\psi}{\partial\zeta}+p_0\frac{\partial^3\psi}{\partial\zeta^3}=0, \tag{23}$$

where $p=sA_\sigma p_0$, $q=p_0q_0$, and

$$q_0=\frac{15}{2V_{\rm p}^6}+\frac{15\eta\mu^3}{2V_{\rm p}^6}-\frac{\mu_1}{2}-\frac{9\mu_1\beta}{2}-\frac{\mu_2\sigma^3}{2}, \tag{24}$$

$$p_0=\frac{V_{\rm p}}{2(\mu_1+\mu_1\beta+\sigma\mu_2)}. \tag{25}$$

Equation (23) is a modified Gardner (MG) equation. The modification is due to the extra term, $(\nu/2\tau)\psi$, which arises due to the effects of the nonplanar geometry. We have already mentioned that $\nu=0$ corresponds to a 1D planar geometry which reduces Eq. (23) to a standard Gardner (SG) equation. Our aim now is to numerically analyze the MG equation. However, for clear understanding, we first briefly discuss the stationary GSs and DL solution of this sG equation (i.e., Eq. (23) with $\nu=0$).

4. Numerical analysis

The exact analytical solution of Eq. (23) is not possible. Therefore, we have numerically solved Eq. (23), and have studied the effects of planar geometry DIA-GSs and DIA-DLs. The stationary SW solution of the SG equation is obtained by considering a moving frame (moving with speed U_0) $\xi = \zeta - U_0\tau$, and imposing all the appropriate boundary conditions for the SW solution, including $\psi \to 0$, $\mathrm{d}\psi/\mathrm{d}\xi \to 0$, and $\mathrm{d}^2\psi/\mathrm{d}\xi^2 \to 0$ at $\xi \to \pm\infty$. These boundary conditions for the stationary Gardner soliton (GS) solution[45] allow us to express the SG equation as

$$\psi = \left[\frac{1}{\psi_{m2}} - \left(\frac{1}{\psi_{m2}} - \frac{1}{\psi_{m1}}\right)\cosh^2\left(\frac{\xi}{\Delta}\right)\right]^{-1}, \tag{26}$$

where

$$\psi_{m1,2} = \psi_m\left[1 \mp \sqrt{1 + \frac{U_0}{V_0}}\right], \tag{27}$$

$$U_0 = \frac{sA_\sigma p_0}{3}\psi_{m1,2} + \frac{q}{6}\psi_{m1,2}^2, \tag{28}$$

$\psi_m = -sA_\sigma/q_0$, $V_0 = A_\sigma^2 s^2 p_0/6q_0$, and the width ($\Delta$) of the Gardner solitons (GSs) is given by

$$\Delta = \sqrt{-\frac{24}{q_0\psi_{m1}\psi_{m2}}}. \tag{29}$$

We note that equation (26) represents an SW solution of Eq. (23) with $\nu = 0$. Therefore, it is obvious that, to have GSs we must have $U_0 < V_0$, otherwise $\psi_{m1,2}$ become imaginary. It is clear from Eq. (15) that the solitary potential profile is positive (negative) if $A > 0$ ($A < 0$). Therefore, $A(\sigma = \sigma_c) = 0$, where σ_c is the critical value of σ above (below) which the SWs with a positive (negative) potential exists, gives the value of σ_c. We have the existence of the small amplitude SWs with a positive potential for $\sigma < \sigma_c$ shown in Figs. 2 and 4 and with a negative potential for $\sigma > \sigma_c$ shown in Figs. 3 and 5.

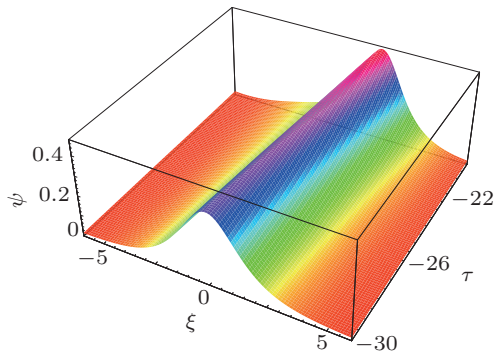


Fig. 2. (color online) The effects of cylindrical geometry ($\nu = 1$) on DIA positive GSs for $U_0 = 0.1$, $\mu = 0.08$, $\alpha = 0.1$, $\mu_1 = 0.5$, $\mu_2 = 0.2$, $\sigma = 9.1$, $s = -1$, and $\mu_d = 0.1$.

The stationary DL solution of the SG equation (23) is obtained by considering a moving frame (moving with speed U_0) $\xi = \zeta - U_0\tau$, and imposing all the appropriate boundary conditions for the DL solution, including $\psi \to 0$, $\mathrm{d}\psi/\mathrm{d}\xi \to 0$, and $\mathrm{d}^2\psi/\mathrm{d}\xi^2 \to 0$ at $\xi \to -\infty$. These boundary conditions for the stationary DL solution[43] allow us to express the SG equation (23) as

$$\psi = \frac{\psi_m}{2}\left[1 + \tanh\left(\frac{\xi}{\Delta}\right)\right], \tag{30}$$

where the amplitude (ψ_m) and the width (Δ) of the DLs, and U_0 are given by

$$\psi_m = s\frac{6U_0}{A_\sigma p_0}, \quad \Delta = \sqrt{-\frac{24}{\psi_m^2 q_0}}, \quad U_0 = -\frac{s^2 A_\sigma^2 p_0}{6q_0}. \tag{31}$$

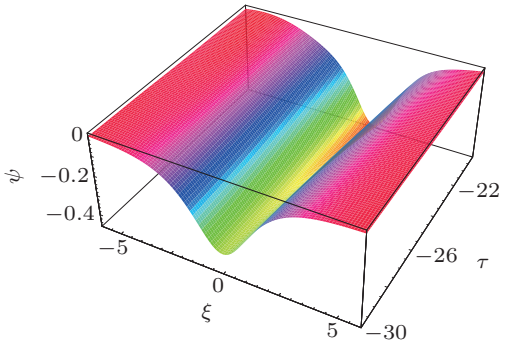


Fig. 3. (color online) The effects of cylindrical geometry ($\nu = 1$) on DIA negative GSs for $U_0 = 0.1$, $\mu = 0.08$, $\alpha = 0.1$, $\mu_1 = 0.5$, $\mu_2 = 0.2$, $\sigma = 9.22$, $s = 1$, and $\mu_d = 0.1$.

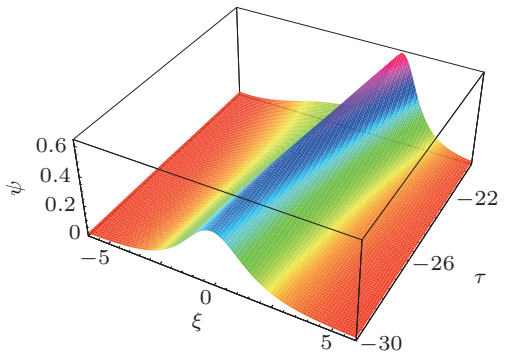


Fig. 4. (color online) The effects of spherical geometry ($\nu = 2$) on DIA positive GSs for $U_0 = 0.1$, $\mu = 0.08$, $\alpha = 0.1$, $\mu_1 = 0.5$, $\mu_2 = 0.2$, $\sigma = 9.1$, $s = -1$, and $\mu_d = 0.1$.

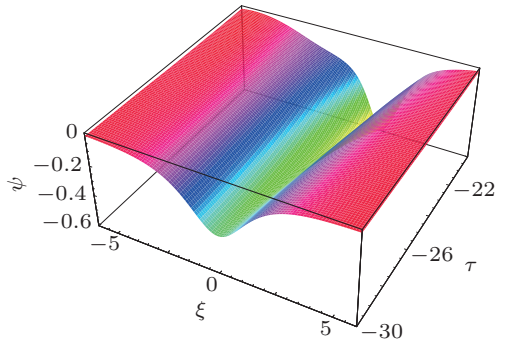


Fig. 5. (color online) The effects of spherical geometry ($\nu = 2$) on DIA negative GSs for $U_0 = 0.1$, $\mu = 0.08$, $\alpha = 0.1$, $\mu_1 = 0.5$, $\mu_2 = 0.2$, $\sigma = 9.22$, $s = 1$, and $\mu_d = 0.1$.

It is clear from Eqs. (30) and (31) that DLs exist if and only if $q_0 < 0$, i.e., $\sigma > \sigma_D$, where σ_D is represented by the $q_0 = 0$ surface plot shown in Fig. 6. Since $p_0 > 0$ and $U_0 > 0$, equations (30) and (31) indicate that the DLs are associated with negative potential if $s = 1$, i.e., $\sigma > \sigma_c$, and associated with positive potential if $s = -1$, i.e., $\sigma < \sigma_c$. It is obvious from Fig. 6 that $\sigma_D > \sigma_c$, which confirms us that DLs are associated with negative potential only. The parametric regimes for the existence of negative DLs are represented by Fig. 6, and DLs exist for parameters corresponding to any point above the $q_0 = 0$ surface plot.

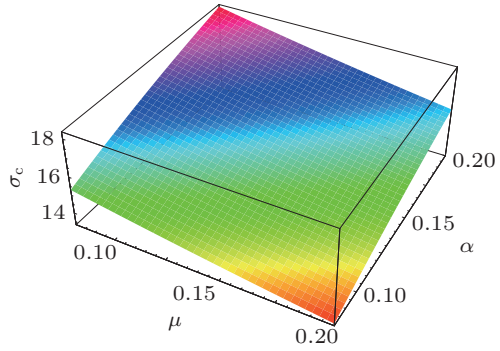


Fig. 6. (color online) Showing the parametric regime for the existence of DLs (obtained from the solutions of $q_0 = 0$ for σ) for $\mu_1 = 0.5$, $\mu_2 = 0.2$, and $\mu_d = 0.1$.

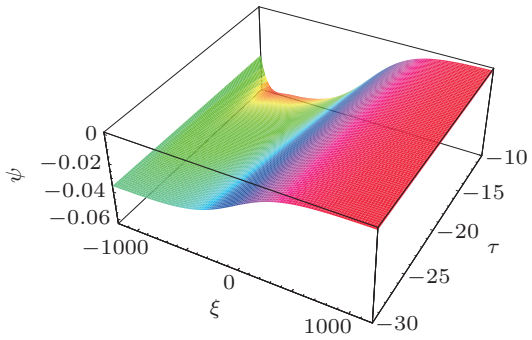


Fig. 7. (color online) The effects of cylindrical geometry on DIA negative DLs for $U_0 = 0.005$, $\sigma = 15.92$, $\mu = 0.08$, $\alpha = 0.1$, $\mu_1 = 0.5$, $\mu_2 = 0.2$, $s = 1$, and $\mu_d = 0.1$.

It may be noted here that the solitary structures are hump or dip shaped non-linear waves of permanent profile whereas DLs can be thought of as an internal sheath separating plasmas at different potential within a plasma system. The profile of DIA SWs beyond the Kortewegde Vries (KdV) limit is mathematically defined as Eq. (26).[48] The double layers are achieved (higher order nonlinear term by balancing dispersion/dissipation) by a bipolar charge distribution. The profile of DLs is mathematically defined as Eq. (30).[51] If we would neglect the higher order nonlinear term (i.e., the fourth term of Eq. (23) or the term containing ψ^3), but would keep the lower order nonlinear term (the third term of Eq. (23) or the term containing ψ^2), we would obtain the solitary structures that are due to the balance between nonlinearity (associated with ψ^2 only) and dispersion.[18,21,51] On the other hand, in our present work, we have kept both the terms containing ψ^2 and ψ^3, and have obtained both SWs (as shown in Figs. 2–5) and DLs (as shown in Figs. 7 and 8).

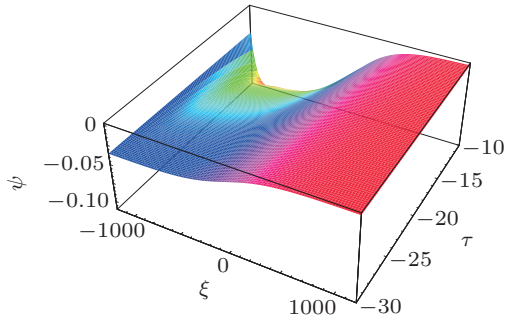


Fig. 8. (color online) The effects of spherical geometry on DIA negative DLs for $U_0 = 0.005$, $\sigma = 15.92$, $\mu = 0.08$, $\alpha = 0.1$, $\mu_1 = 0.5$, $\mu_2 = 0.2$, $s = 1$, and $\mu_d = 0.1$.

We have numerically solved Eq. (23), and have studied the effects of nonplanar geometries on time-dependent DIA-SWs and DIA-DLs. The initial condition that we have used in our numerical analysis is in the form of the stationary solution of Eq. (23) without the term $(\nu/2\tau)\psi$. The results are depicted in Figs. 2–8. Figures 2 (4) and 3 (5) show how the effects of a cylindrical (spherical) geometry modify the DIA-GSs. The numerical solutions of Eq. (23) (displayed in Figs. 2–8) reveal that for a large value of τ (e.g., $\tau = -30$), the cylindrical ($\nu = 1$) and spherical ($\nu = 2$) DIA-SWs are almost similar to 1D planar ($\nu = 0$) structures. This is because for a large value of τ, the term $(\nu/2\tau)\psi$, which is due to the effects of the cylindrical or spherical geometry, is no longer dominant. However, as the value of τ decreases, the term $(\nu/2\tau)\psi$ becomes dominant, and spherical and cylindrical DIA-SWs structures differ from 1D planar ones. It is found that as the value of τ decreases, the amplitude of these localized pulses increases. Furthermore, the cylindrical SWs travel faster than the 1D SWs but slower than the spherical ones, and that the amplitude of cylindrical DIA-SWs structure is larger than those of 1D planar ones, but smaller than that of the spherical ones.

5. Discussion

We have considered the nonlinear propagation of DIA waves in a plasma system consisting of inertial positive and negative ions, Maxwellian cold electrons, non-thermal hot electrons, and negatively charged static dust. The reductive perturbation method has been employed in order to derive the MG equation which is valid beyond the K–dV limit (corresponding to the vanishing of the nonlinear coefficient of the K–dV equation, i.e., $\sigma \sim \sigma_c$ in our present situation). The results discovered from the numerical solutions of the MG equation can be given briefly below.

First, the DENP system under consideration supports the finite amplitude GSs and DLs, whose basic features (polarity, amplitude, width, etc.) depend on the temperature ratio of two electrons, dust density, and ion densities.

Second, the GSs represented by Eq. (26) for planar geometry and steady state condition are found to be significantly different from the K–dV solitons represented in the form of $\mathrm{sech}^2(\xi/\Delta)$, which do not exist for $\sigma \sim \sigma_c$.

Third, GSs are shown to exist around $\sigma = \sigma_c$, and are found to be different from the K–dV solitons, which do not exist around $\sigma = \sigma_c$. We note that $\sigma_c = 9.210$ for $\mu = 0.08$, $\alpha = 0.1$, $\mu_1 = 0.5$, $\mu_2 = 0.2$, and $\mu_d = 0.1$.

Fourth, at $\sigma < \sigma_c$, positive GSs exist, and at $\sigma > \sigma_c$, negative GSs exist.

Fifth, it is also found that the magnitude of the amplitude of positive and negative GSs decreases with σ and increases with U_0.

Sixth, the width of positive and negative GSs decreases with σ and U_0.

Seventh, the DLs having large width and negative potential, exist for $\sigma > \sigma_c$, and no positive DLs are formed. We note that $\alpha_D = 15.908$ for $\mu = 0.08$, $\alpha = 0.1$, $\mu_1 = 0.5$, $\mu_2 = 0.2$, and $\mu_d = 0.1$.

Eighth, the magnitude of the amplitude of DLs increases with the increase of σ and U_0. The width of positive DLs increases with both σ and U_0.

Ninth, the numerical analysis of the MG equation indicates that for a very large value of τ, the nonplanar DIA-DLs are identical, but the magnitude of the amplitude of both cylindrical and spherical DIA-DLs increases with the increase of the magnitude of τ.

Tenth, the amplitude of the cylindrical DIA-SWs and DIA-DLs are larger than those of 1D ones, but smaller than that of the spherical ones.

In our numerical analysis, we have used a wide range of the plasma parameters ($\mu = 0.1 - 0.9$, $\mu_1 = 0.1 - 0.9$ $\mu_2 = 0.1 - 0.9$, $\sigma = 10 - 13$, and $\alpha = 0.1 - 0.5$) that are relevant to both space and laboratory plasmas.[14,16,17,39]

It may be stressed here that the results of this investigation could be useful for understanding the nonlinear features of electrostatic disturbances in laboratory[38] and space plasmas,[30,33] particularly in noctilucent cloud region in Earths atmosphere,[34] at the edges of the Auroral Kilometric Radiation source region,[53] Saturns E-ring, double-plasma machines,[35] hot turbulent thermonuclear plasma,[37] rf discharge plasma,[54] etc, where electrons of different kinds involving thermal effects are the major plasma species. Our present investigation comprising of DIA SWs and DLs in nonplanar dusty plasma system is limited to small but finite amplitude SWs.

It may also be added here that the analysis of small or large amplitude double layers, vortices, shocks, etc, would be essential to describe the localized nonlinear perturbations of such laboratory and space plasma but beyond the scope of our present investigation.

References

[1] Vender D, Stoffels W W, Stoffels E, Kroesen G M W and de Hoog F J 1995 *Phys. Rev. E* **51** 2436
[2] Kimura T, Imagaki K and Ohe K 1998 *J. Phys. D* **31** 2295
[3] Berezhnoj S V, Shin C B, Buddemeier U and Kaganovich I 2000 *Appl. Phys. Lett.* **77** 800
[4] Franklin R N 2002 *Plasma Sources Sci. Technol.* **11** 31
[5] Rahman O, Mamun A A and Ashrafi K S 2011 *Astrophys. Space Sci.* **335** 425
[6] Zou X, Liu H P, Qiu M H and Sun X H 2011 *Chin. Phys. Lett.* **28** 125201
[7] ZOU X, Liu J Y, Wang Z X, Gong Y, Liu Y and Wang X G 2004 *Chin. Phys. Lett.* **21** 1572
[8] Lieberman M A and Lichtenberg A 2005 *Principle of Plasma Discharges and Materials Processing* (New York: Wiley)
[9] Jacquinot J, McVey B D and Scharer J E 1977 *Phys. Rev. Lett.* **39** 88
[10] Weingarten A, Arad R, Maron Y and Fruchtman A 2001 *Phys. Rev. Lett.* **87** 115004
[11] Ichiki R, Yoshimura S, Watanabe T, Nakamura Y and Kawai Y 2002 *Phys. Plasmas* **9** 4481
[12] Meige A, Plihon N, Hagelaar G J M, Boeuf J P, Chabert P and Boswell R W 20007 *Phys. Plasmas* **14** 053508
[13] Coates A J, Crary F J, Lewis G R, Young D T, Waite J H and Sittler E C 2007 *Geophys. Res. Lett.* **34** 22103
[14] Plihon N and Chabert P 2011 *Phys. Plasmas* **18** 082102
[15] Shukla P K and Eliasson B 2009 *Rev. Mod. Phys.* **81** 25
[16] Kim S H and Merlino R L 2006 *Phys. Plasmas* **13** 052118
[17] Merlino R L and Kim S H 2006 *Appl. Phys. Lett.* **89** 091501
[18] Mamun A A, Cairns R A and Shukla P K 2009 *Phys. Lett. A* **373** 2355
[19] Ghim Y and Hershkowitz N 2009 *Appl. Phys. Lett.* **94** 151503
[20] Mamun A A, Shukla P K and Eliasson B 2009 *Phys. Rev. E* **80** 046406
[21] Mamun A A, Shukla P K and Eliasson B 2009 *Phys. Plasmas* **16** 114503
[22] Hussain S, Akhtar N and Saeed-ur-Rehman 2011 *Chin. Phys. Lett.* **28** 045202
[23] Cairns R A, Mamun A A, Bingham R, Boström R, Dendy R O, Nairns C M C and Shukla P K 1995 *Geophys. Res. Lett.* **22** 2709
[24] Boström R 1992 *IEEE Trans. Plasma Sci.* **20** 756
[25] Dovner P O, Eriksson A I, Bostrom R and Holback B 1994 *Geophys. Res. Lett.* **21** 1827
[26] Gill T S, Bala P, Kaur H, Saini N S, Bansal S and Kaur J 2004 *Eur. Phys. J. D* **31** 91
[27] Sabry R, Moslem W M and Shukla P K 2009 *Phys. Plasmas* **16** 032302
[28] Jones W D, Lee A, Gleman S M and Doucet H J 1975 *Phys. Rev. Lett.* **35** 1349
[29] Ghosh K K, Paul B and Paul S N 2008 *J. Phys. A: Math. Theor.* **41** 335501
[30] Geiss J, Balsiger H, Eberhardt P, Walker H P, Weber L and Young D T 1978 *Space Sci. Rev.* **22** 537
[31] Song S B, Chang C S and Duk-In Choi 1997 *Phys. Rev. E* **55** 1
[32] Lakhina G S, Kakad A P, Singh S V and Verheest F 2008 *Phys. Plasmas* **15** 062931
[33] Dubouloz N, Treumann R A, Pottelette R and Malingre M 1993 *Geophys. Res. Lett.* **98** 17415
[34] Shah A, Haque Q and Mahmood S 2009 *Phys. Plasmas* **16** 123704
[35] Spileman R B, Degroot J S and Rasmuseen D A 1976 *J. Plasma Phys.* **47** 1909
[36] Morals G J and Lee Y C 1974 *Phys. Rev. Lett.* **33** 1534
[37] Estabrook K and Krueer W I 1978 *Phys. Rev. Lett.* **40** 42
[38] Oleson N L and Found F G 1946 *J. Appl. Phys.* **29** 416
[39] Sheridan T E, Goeckner M J and Goree J 1991 *J. Vac. Sci. Technol A* **9** 3
[40] Shukla P K and Rosenberg M 1999 *Phys. Plasmas* **6** 1038
[41] Miura R M, Gardner C S and Kruskal M D 1968 *J. Math. Phys.* **9** 1204
[42] Lee N C 2009 *Phys. Plasmas* **16** 042316
[43] Mamun A A and Mannan A 2011 *JETP Lett.* **94** 356

[44] Hossain M M, Mamun A A and Ashrafi K S 2011 *Phys. Plasmas* **18** 103704
[45] Mannan A and Mamun A A 2011 *Phys. Rev. E* **84** 026408
[46] Asaduzzaman M and Mamun A A 2012 *Astrophys. Space Sci.* **341** 535
[47] Ghosh D K, Chatterjee P and Ghosh U N 2012 *Phys. Plasmas* **19** 033703
[48] Shuchy S T, Mannan A and Mamun A A 2012 *JETP Lett.* **95** 310
[49] Masud M M, Assaduzzaman M and Mamun A A 2013 *Astrophys. Space Sci.* **343** 221
[50] Akhter T, Hossain M M and Mamun A A 2013 *Astrophys. Space Sci.* **344** 105
[51] Hossain M M and Mamun A A 2012 *J. Phys. A: Math. Theor.* **45** 125501
[52] Washimi H and Taniuti T 1966 *Phys. Rev. Lett.* **17** 996
[53] Ergun R E, Carlson C W, McFadden J P, Mozer F S, Delory G T, Peria W, Chaston C C, Temerin M, Elphic R, Strangeway R, Pfaff R, Cattell C A, Klumpar D, Shelley E, Peterson W, Moebius E and Kistler L 1998 *Geophys. Res. Lett.* **25** 2061
[54] Nishida Y and Nagasawa T 1986 *Phys. Fluids* **29** 345
[55] Shukla P K and Silin V P 1992 *Phys. Scripta* **45** 508
[56] Mamun A A and Shukla P K 2002 *Phys. Plasmas* **9** 1468
[57] Mamun A A and Shukla P K 2002 *IEEE. Trans. Plasma Sci.* **30** 720
[58] Ghosh S and Bharuthram R 2008 *Astrophys. Space Sci.* **314** 121